

Quasiparticle relaxation dynamics in spin-density-wave and superconducting $\text{SmFeAsO}_{1-x}\text{F}_x$ single crystals

T. Mertelj¹, P. Kusar¹, V.V. Kabanov¹, L. Stojchevska¹, N.D. Zhigadlo², S.

Katrych², Z. Bukowski², J. Karpinski², S. Weyeneth³ and D. Mihailovic¹

¹*Complex Matter Dept., Jozef Stefan Institute, Jamova 39, Ljubljana, SI-1000, Ljubljana, Slovenia*

²*Laboratory for Solid State Physics, ETH Zürich, 8093 Zürich, Switzerland and*

³*Physik-Institut der Universität Zürich, 8057 Zürich, Switzerland*

(Dated: February 4, 2022)

We investigate the quasiparticle relaxation and low-energy electronic structure in undoped SmFeAsO and near-optimally doped $\text{SmFeAsO}_{0.8}\text{F}_{0.2}$ single crystals - exhibiting spin-density wave (SDW) ordering and superconductivity respectively - using pump-probe femtosecond spectroscopy. In the undoped single crystals a single relaxation process is observed, showing a remarkable critical slowing down of the QP relaxation dynamics at the SDW transition temperature $T_{SDW} \simeq 125\text{K}$. In the superconducting (SC) crystals multiple relaxation processes are present, with distinct SC state quasiparticle recombination dynamics exhibiting a BCS-like T -dependent superconducting gap, and a pseudogap (PG)-like feature with an onset above 180K indicating the existence of a pseudogap of magnitude $2\Delta_{PG} \simeq 120\text{ meV}$ above T_c . From the pump-photon energy dependence we conclude that the SC state and PG relaxation channels are independent, implying the presence of two separate electronic subsystems. We discuss the data in terms of spatial inhomogeneity and multi-band scenarios, finding that the latter is more consistent with the present data.

The discovery of high-temperature superconductivity in iron-based pnictides (IP)¹⁻³ has attracted a great deal of attention recently. Contrary to the cuprate superconductors, where a single band with a high degree of correlations is believed to be sufficient starting point for the description of the electronic properties, there is a clear theoretical⁴ and experimental⁵ evidence that in IP several bands cross the Fermi energy (ϵ_F).⁵⁸ The implications of the presence of several bands at ϵ_F in IP are still under intense investigation. In the undoped state two SDW gaps were detected by optical spectroscopy⁶ in 122 compounds (AFe_2As_2 A=Ba,Sr) presumably originating from different bands crossing ϵ_F . In LaFeAsO (La-1111) a similar optical conductivity suppression was observed⁷, but no analysis in terms of SDW gaps was performed. In the superconducting state multiple superconducting gaps were detected⁸⁻¹¹ corresponding to different bands crossing ϵ_F . In addition to superconducting gaps also the presence of a pseudogap was reported by NMR^{12,13} and point-contact Andreev spectroscopy¹⁴ in La-1111.

Time resolved spectroscopy has been very instrumental in elucidating the nature of the electronic excitations in superconductors, particularly cuprates, by virtue of the fact that different components in the low-energy excitation spectrum could be distinguished by their different lifetimes¹⁵⁻²⁹. Moreover, the relaxation kinetics can give us valuable information on the electronic density of states¹⁶ and electron-phonon coupling³⁰. Extensive and systematic experiments on cuprates have also given information on the behavior of the pseudogap for charge excitations, complementing the information obtained on spin excitations from NMR and other spectroscopies^{17,19,25}.

In this work we present a time-resolved femtosecond spectroscopy study of undoped and near-optimally doped $\text{SmFeAsO}_{1-x}\text{F}_x$ single crystals with $x = 0$ and $x \simeq 0.2$ with the aim of elucidating the low energy elec-

tronic structure, investigating possible multi-component response as a sign of phase separation and to obtain detailed information about the quasiparticle (QP) dynamics in the normal, SDW and superconducting states.

I. EXPERIMENTAL

Optical experiments were performed using the standard pump-probe technique, with 50 fs optical pulses from a 250-kHz $\text{Ti:Al}_2\text{O}_3$ regenerative amplifier seeded with an $\text{Ti:Al}_2\text{O}_3$ oscillator. We used the pump photons with either doubled ($\hbar\omega_P = 3.1\text{ eV}$) or fundamental ($\hbar\omega_P = 1.55\text{ eV}$) photon energy and the probe photons with 1.55 eV photon energy. The pump and probe polarizations were perpendicular to each other and oriented with respect to the the crystals to obtain the maximum amplitude of the response at low temperatures. The pump and probe beam diameters were determined by measuring the transmittance of calibrated pinholes mounted at the sample place³¹.

The crystals were flux grown at high pressure at ETH in Zurich³² and were approximately $\sim 120 \times \sim 80\text{ }\mu\text{m}$ in size. For optical measurements the crystals were glued on a sapphire window mounted in an optical liquid-He flow cryostat.

A. Undoped, spin-density-wave ordered SmFeAsO

In Fig. 1 we plot temperature dependence of $\Delta R/R$ transients in undoped SmFeAsO . The only discernible difference of the response at different pump-photon energies is the presence of a coherent phonon oscillation with the frequency 5.1 THz (170 cm^{-1}) at 295K , at $\hbar\omega_P = 1.55$

eV, which is absent at $\hbar\omega_P = 3.1$ eV, consistent with Raman data³³. Apart of the coherent phonon oscillation the transients consist from a negative-amplitude single-exponential relaxation with a temperature independent rise time of ~ 180 fs (see Fig. 2 (a)). Around ~ 125 K an additional long lived response appears with decay time beyond our measurement delay range. The amplitude of the transients, A_0 , linearly increases with decreasing temperature down to ~ 170 K (see Fig. 2 (c)) with the relaxation time, τ_{ud} , of ~ 220 fs time being virtually constant above 200K. Below 200 K τ_{ud} starts to increase while the amplitude starts to depart from the linear dependence only below ~ 170 K rapidly increasing below ~ 140 K, and achieving a maximum at 115 K, upon entering the SDW state. With further decrease of the temperature the amplitude slightly drops at first and then remains constant below 50 K. Simultaneously with the maximum of the amplitude τ_{ud} shows a remarkable divergent-like peak at ~ 120 K and then drops to a temperature independent value of 0.8 ps below 50 K.

The rise and decay times are virtually independent of the fluence, \mathcal{F} , at all temperatures (see Fig. 3) while the amplitude increases linearly with \mathcal{F} at 295K and shows a weak saturation above $\mathcal{F} = 25 \mu\text{J}/\text{cm}^2$ at 5K.

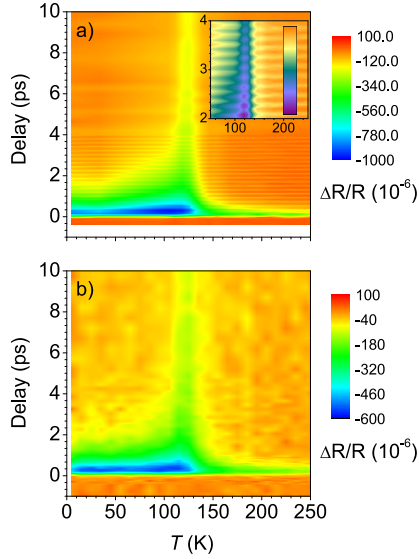


Figure 1: $\Delta R/R$ transients as a function of temperature at 1.55 eV pump-photon energy and $18 \mu\text{J}/\text{cm}^2$ (a) and 3.1 eV pump-photon energy and $15 \mu\text{J}/\text{cm}^2$ (b) in undoped SmFeAsO. In (a) the coherent phonon, shown expanded in the insert, is artificially smeared beyond 4 ps delay due to a decreased time resolution of scans.

B. Superconducting SmFeAsO_{0.8}F_{0.2}

The temperature dependence of the $\Delta R/R$ -transients in the near optimally doped sample is shown in Fig. 4. Contrary to the undoped case the transients show complex time and temperature dependencies. Independent of

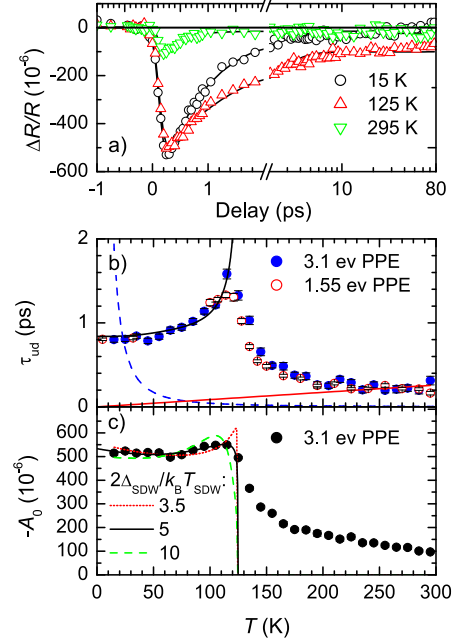


Figure 2: $\Delta R/R$ transients at representative temperatures in undoped SmFeAsO with single-exponential decay fits (a). The relaxation time at two pump photon energies b) and amplitude (c) as functions of temperature at $\mathcal{F} = 15 \mu\text{J}/\text{cm}^2$. The red solid line in (b) is fit of equation (1) to τ_{ud} above 230K. The blue dashed line in (b) is equation (2) with $\lambda = 0.2$ and $\Theta_D = 175\text{K}$. Black thin solid line in (a) represents the fit of equation (28) from¹⁶ discussed in detail in text. Thin lines in (b) represent the fits of equation (6) from¹⁶ with different magnitudes of the gap.

the $\hbar\omega_P$ one can clearly resolve three temperature regions with different characteristic behaviors.

(i) At the high temperatures a negative transient is observed with initial 0.25-ps decay followed by a slower response consisting from a weak peak at 12 ps (see Fig. 5 (a)) at $\hbar\omega_P = 3.1$ eV. The transients linearly scale with increasing fluence except in the region of the initial 0.25-ps decay where a weak \mathcal{F} -dependence is observed at low \mathcal{F} . At $\hbar\omega_P = 3.1$ eV the transients have the same shape and similar amplitude as in undoped SmFeAsO without the coherent phonon. At $\hbar\omega_P = 1.55$ eV the negative high- T transients are much weaker than at $\hbar\omega_P = 3.1$ eV so only the initial 0.25-ps decay is resolved from the noise (see Fig. 6). In addition a coherent phonon is observed with a softer frequency than in undoped SmFeAsO of 4.6 THz (153 cm^{-1}) having similar amplitude at both $\hbar\omega_P$.

(ii) At the intermediate temperatures above T_c and low \mathcal{F} the transients are positive on the sub-ps timescale cross zero around 4 ps with slow dynamics similar to the high-temperature one. At high \mathcal{F} the positive part of the transients vanishes and the transients become qualita-

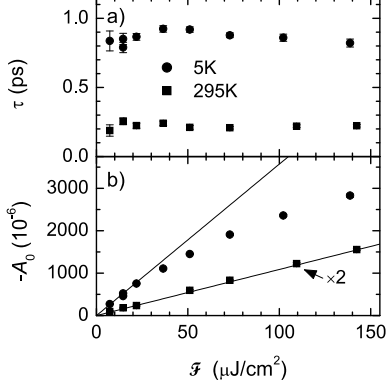


Figure 3: Fluence dependence of the $\Delta R/R$ transient amplitude and relaxation time in undoped SmAsFeO at two different temperatures.

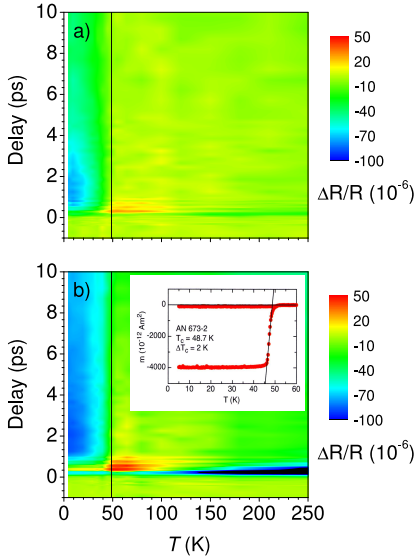


Figure 4: $\Delta R/R$ transients as a function of temperature at 1.55-eV pump-photon energy (a) and 3.1-eV pump-photon energy (b) in superconducting SmFeAsO_{0.8}F_{0.2}. The pump fluence was $17 \mu\text{J}/\text{cm}^2$ at 3.1 eV and $15 \mu\text{J}/\text{cm}^2$ at 1.55 eV. Below T_c the response of the superconducting state is clearly seen. The temperature dependence of the magnetization is shown in the inset.

tively identical to those at higher temperatures (see Fig. 5). The only remaining difference is a delay-independent positive vertical shift of the the intermediate T scans with respect to those measured at 250 K and an increased coherent phonon frequency of 5.1 THz (170 cm^{-1}). The $\hbar\omega_P = 1.55\text{-eV}$ transients are, as at higher temperatures, similar to the $\hbar\omega_P = 3.1\text{-eV}$ transients but weaker.

(iii) Below T_c an additional negative component appears with a rise time of 0.2-0.6 ps, depending on the $\hbar\omega_P$ and pump fluence, and decay time of ~ 5 ps. The com-

ponent has a similar amplitude at both $\hbar\omega_P$. At high \mathcal{F} the additional negative component becomes undetectable due to a saturation and the transients become virtually identical to those measured at 55 K including the coherent phonon response.

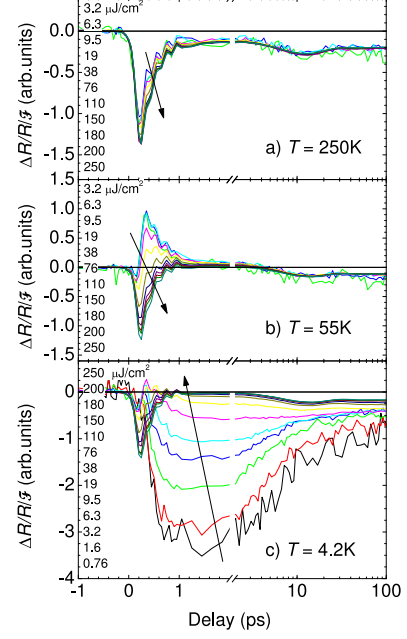


Figure 5: Normalized $\Delta R/R$ transients at selected temperatures at 3.1-eV pump photon energy as a function of \mathcal{F} in superconducting SmFeAsO_{0.8}F_{0.2}. Above $\sim 150 \mu\text{J}/\text{cm}^2$ the traces start to overlap indicating a linear \mathcal{F} -dependence. The arrows indicate the direction of increasing \mathcal{F} .

II. DISCUSSION

A. Undoped SmFeAsO

Upon cooling undoped LaFeAsO undergoes a sequence of a structural transition from a tetragonal to orthorhombic symmetry, at $T_s = 156\text{K}$, and a magnetic SDW transition at $T_{\text{SDW}} = 138\text{K}$.³⁴ In SmFeAsO $T_{\text{SDW}} \sim 135\text{K}$ ³⁵ while the structural transition was reported at lower temperature $T_s = 130\text{K}$.³⁶ So far due to possible different oxygen deficiencies in the two experiments^{35,36} and strong doping dependence of both T_{SDW} and T_s it was not possible to reliably distinguish between T_{SDW} and T_s in SmFeAsO. Our data show a marked critical slowing down at 125K (see Fig. 1) in the form of the long-lived relaxation tail, while the initial picosecond exponential decay time shows a maximum at $\sim 115\text{K}$. Since the long-lived relaxation tail affects the quality of the single-exponential picosecond fit (see Fig. 2(a)) we can not reliably identify 115 K as a separate transition temperature. We are

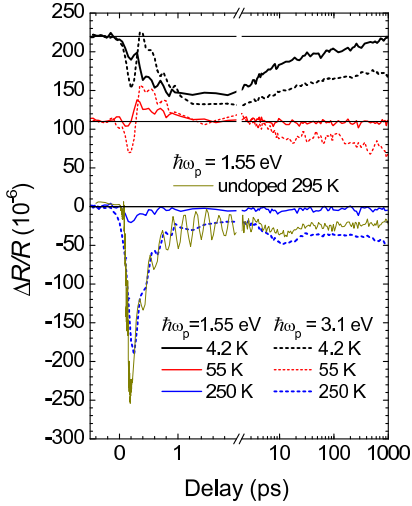


Figure 6: $\Delta R/R$ transients at different pump-photon energies and selected temperatures in superconducting $\text{SmFeAsO}_{0.8}\text{F}_{0.2}$. For comparison the 295 K transient from undoped SmFeAsO is also shown.

therefore unable to differentiate between the structural and spin transitions so we will only refer to a single transition temperature $T_{\text{SDW}} \approx T_s \approx 125$ K in the rest of the paper.

From our data T_{SDW} is lower than reported in literature^{35,37}. The apparent lower T_{SDW} can originate in an elevated temperature of the excited volume with respect to the cryostat temperature due to the laser heating. The ~ 10 -K shift of T_{SDW} is larger than the shift of T_c of a few (2-3) K observed in the superconducting crystals under similar excitation conditions. Due to a variable thermal coupling to the sapphire substrate for such small crystals a small decrease of T_{SDW} originating from the oxygen deficiency can not be distinguished from the laser heating in our samples.

Above T_{SDW} undoped pnictides are bad metals with resistivities in the $\text{m}\Omega\text{cm}$ range^{7,38} and plasma frequency in an ~ 1 eV range^{6,7}. The $\Delta R/R$ transients in this temperature range are therefore attributed to the relaxation of electrons in the states near ϵ_F and can be analyzed by means of the recent theoretical results³⁰ on electron relaxation in metals. The \mathcal{F} -independent relaxation time warrants use of the low excitation expansion³⁰, where in the high temperature limit the relaxation time is proportional to the temperature,³⁹

$$\tau = \frac{2\pi k_B T}{3\hbar\lambda\langle\omega^2\rangle}. \quad (1)$$

Here $\lambda\langle\omega^2\rangle$ is the second moment of the Eliashberg function³⁰, λ the electron-phonon coupling constant and k_B the Boltzman constant. In the low temperature limit the relaxation time is predicted to diverge at low T :³⁰

$$\tau = \frac{2\hbar\Theta_D}{\pi^3\lambda k_B T^2}, \quad (2)$$

where Θ_D is the Debye temperature. From the fit of equation (1) to the relaxation time above 230 K (see Fig. 2) we obtain $\lambda\langle\omega^2\rangle = 135 \pm 10 \text{ meV}^2$. If we estimate $\langle\omega^2\rangle \approx 25^2 \text{ meV}^2$ from inelastic neutron data⁴⁰ we obtain $\lambda \approx 0.2$ indicating a rather weak electron phonon coupling, which can not explain high T_c in the doped compound within a single band BCS model. However, owing to the multiband nature of iron-pnictides it is possible, that due to optical selection rules some bands with possible higher couplings are not detected by $\Delta R/R$ transients. To check the consistency of the resulting value of λ we plot in Fig. 2 (b) also the low- T result (2) indicating validity of the high- T approximation (1) above 230K.

Below T_{SDW} a gap opens at the Fermi surface introducing a bottleneck in the relaxation. The relaxation across a temperature dependent gap was analyzed by Kabanov *et al.*¹⁶ We use equation (6) from Kabanov *et al.*¹⁶, which describes the photo-excited change in quasiparticle density in the presence of a temperature dependent gap, to fit the amplitude below $T_{\text{SDW}} = 125$ K. Using a single SDW gap energy with the BCS temperature dependence and $2\Delta_{\text{SDW}}/k_B T_{\text{SDW}} \simeq 5$ results in a rather good fit to the amplitude temperature dependence (see Fig. 2 (c)). Equation (28) for the relaxation time from Kabanov *et al.*¹⁶ with the same $\Delta_{\text{SDW}}(T)$ describes well also the temperature dependence of the relaxation time (see Fig. 2 (c)). However, equation (28) from Kabanov *et al.*¹⁶ also predicts a fast decrease of the relaxation time with \mathcal{F} , which is not observed in our data. The reason for this might originate in the fact that the SDW state is not fully gaped and the energy relaxation is not limited by the anharmonic energy transfer from the high frequency to the low frequency phonons as assumed in the derivation.¹⁶

B. Decomposition of the $\Delta R/R$ transients in superconducting $\text{SmFeAsO}_{0.8}\text{F}_{0.2}$ into components.

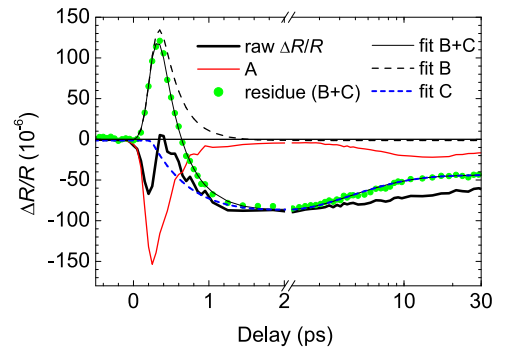


Figure 7: Decomposition of $\Delta R/R$ transients into different components in superconducting $\text{SmFeAsO}_{0.8}\text{F}_{0.2}$.

While the transients in the undoped sample show a simple single-exponential relaxation, which is sensitive to the phase transition to the orthorhombic SDW state, the transients in the doped sample show a clear multicompo-

nent relaxation. To separate contributions from different components we use^{41,42} the fluence dependence of the reflectivity transients. The data can be consistently described by three distinct components A, B and C, which are tightly connected with three observed temperature regions.

The temperature-independent linear scaling of the transients with \mathcal{F} above $\sim 150 \mu\text{J}/\text{cm}^2$ suggests the decomposition of the raw $\Delta R/R$ into component A which scales linearly with \mathcal{F} and a *residue* which saturates at finite \mathcal{F} (see Fig. 7). Component A dominates at high temperatures and has to originate in at least three distinct relaxation processes due to the relatively complex time evolution. (i) The slower dynamics, which is virtually the same as in undoped SmFeAsO at high temperatures (see Fig. 6), could be attributed to the band renormalization due to the lattice expansion. (ii) The sub-ps decay, also having a similar decay time as in undoped SmFeAsO at high temperatures, will be discussed in more detail below. (iii) The oscillatory part of component A is attributed to a coherent phonon oscillation which appears softer as in undoped SmFeAsO. Except for the shift of the coherent phonon frequency all show only a minor T -dependence.

The *residue* shows an unipolar single-exponential decay (see Fig. 8) above T_c , which we name component B. Component B dominates in the raw transients in the intermediate temperature range, above T_c . Below T_c the *residue* changes to a bipolar multi-exponential decay, evidently due to the appearance of an additional relaxation process associated with the superconducting state named component C. Component C saturates at lower $\mathcal{F} \approx 10 \mu\text{J}/\text{cm}^2$ than component B, which saturates above $\sim 70 \mu\text{J}/\text{cm}^2$. The decomposition to the three components is further supported by comparison of the raw $\Delta R/R$ at different $\hbar\omega_P$ shown in Fig. 6 where components A and B show much smaller amplitudes at $\hbar\omega_P = 1.55 \text{ eV}$ in comparison to $\hbar\omega_P = 3.1 \text{ eV}$, while the amplitude of component C shows a negligible $\hbar\omega_P$ dependence.

Above T_c we fit the *residue* with a single exponential decay (component B)⁴³ (see Fig. 8),

$$\frac{\Delta R_B}{R} = \frac{A_B}{2} e^{-\frac{t-t_0}{\tau_B}} \text{erfc}\left(\frac{\sigma^2 - 4(t-t_0)\tau_B}{2\sqrt{2}\sigma\tau_B}\right), \quad (3)$$

where σ corresponds to the effective width of the excitation pulse with a Gaussian temporal profile arriving at t_0 and τ_B the exponential relaxation time. Below T_c additional exponential decays representing component C are needed to fit the *residue*,

$$\begin{aligned} \frac{\Delta R_C}{R} = & A_{1C} \left(e^{-\frac{t-t_0}{\tau_{1C}}} - e^{-\frac{t-t_0}{\tau_{iC}}} \right) \\ & + A_{2C} \left(e^{-\frac{t-t_0}{\tau_{2C}}} - e^{-\frac{t-t_0}{\tau_{iC}}} \right) \end{aligned} \quad (4)$$

where τ_{iC} represents the rise time and τ_{iC} the decay times. The resulting fit parameters for component B are shown in Fig. 9. The decay time, $\tau_{1B} \approx 0.25 \text{ ps}$ at 4

K, slightly increases with increasing temperature below 200 K. Above 200 K, where artifacts due to subtraction of component A start to be significant, τ_{1B} steeply increases towards 1 ps. The amplitude of component B, A_B , stays almost constant up to $\sim 70 \text{ K}$ and then drops monotonously.

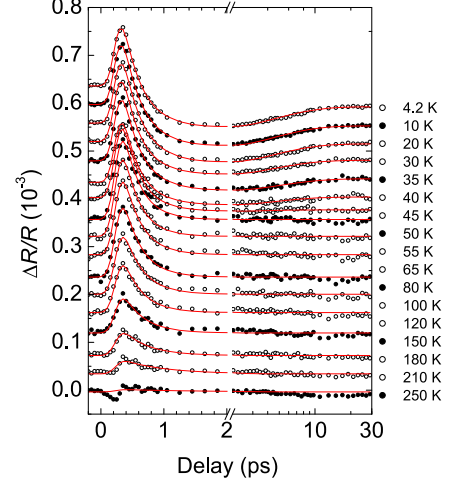


Figure 8: Temperature dependence of $\Delta R/R$ transients with component A subtracted. Thin lines are single exponential decay fits (component B) above T_c and multi-exponential decay fits (a sum of component B and C) below T_c .

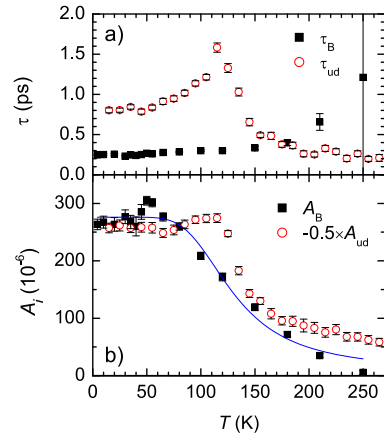


Figure 9: Temperature dependence of the component-B relaxation time (a) and amplitude (b) in superconducting SmAsFeO_{0.8}F_{0.2} obtained from the fits. The thin line is the fit for the case of a relaxation over a T -independent gap^{16,41} with $2\Delta_{PG} = 120 \text{ meV}$. For comparison, the temperature dependence of the relaxation time and the transient amplitude in undoped SmAsFeO is also shown.

C. Superconducting response in $\text{SmFeAsO}_{0.8}\text{F}_{0.2}$

For easier separation of component C associated with the superconducting response we use the fact that components A and B are temperature independent in the superconducting state. We therefore extract component C by subtracting the average of transients measured at 55 and 65 K from transients measured below 55 K. The subtracted transients clearly show a two-step decay with a finite rise time and are excellently fit by equation (4) as shown in Fig. 10.

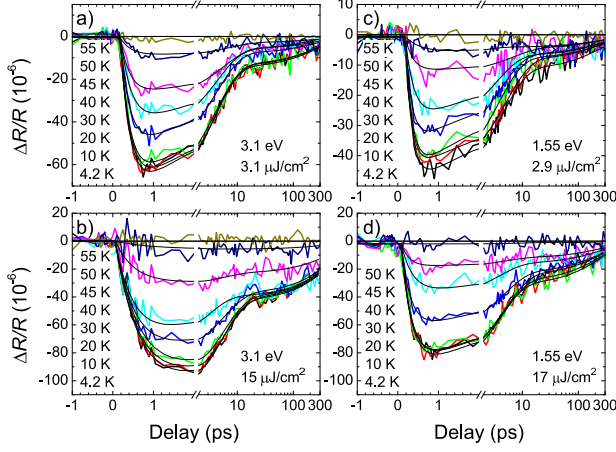


Figure 10: Component C as a function of temperature at different pump photon energies and fluences. Thin lines are fits discussed in text.

In the spirit of the Rotwarf-Taylor model²⁷ we associate the rise time with establishment of the thermal quasi-equilibrium between the photo-excited quasiparticles and high frequency ($\hbar\omega > 2\Delta_{\text{SC}}$) phonons. The shorter relaxation time is associated with establishment of the local thermal equilibrium between all degrees of freedom, while the longer relaxation time is due to energy escape out of the probed volume. This is supported by increased relative amplitude of the long decay with respect to the total amplitude at higher \mathcal{F} .

Neither the rise time nor the relaxation times (see Fig. 11) show any temperature dependence within experimental error, while only τ_{TC} shows dependence on \mathcal{F} and $\hbar\omega_{\text{P}}$. τ_{TC} is always faster at $\hbar\omega_{\text{P}} = 1.55$ eV and shows much weaker \mathcal{F} -dependence than at $\hbar\omega_{\text{P}} = 3.1$ eV, where it increases from 0.3 ps at $\mathcal{F} = 3 \mu\text{J}/\text{cm}^2$ to 0.6 ps at $\mathcal{F} = 15 \mu\text{J}/\text{cm}^2$. While an increase of τ_{TC} with increasing $\hbar\omega_{\text{P}}$ is expected due to the photo-excitation being farther away from ϵ_{F} an increasing \mathcal{F} -dependence with increasing $\hbar\omega_{\text{P}}$ is not completely understood.

In Fig. 12 we plot \mathcal{F} -dependence of the component C amplitude, A_{SC} . Similarly as in the cuprates³¹ the response saturates with increasing \mathcal{F} indicating a complete destruction of the superconducting state in the excited volume. By taking into account the effects of inhomogeneous excitation due to finite penetration depths and beam diameters³¹ we determine the threshold ex-

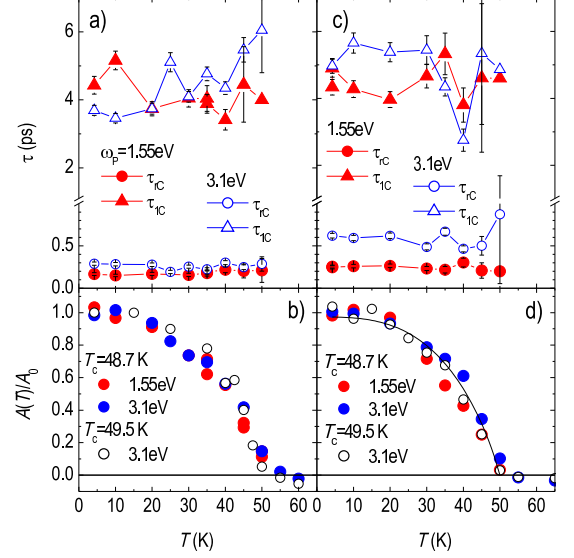


Figure 11: Rise time and relaxation time (a), (c) and amplitude (b), (d) of component C as functions of temperature at $\mathcal{F} = 2.9 \mu\text{J}/\text{cm}^2$ and $3 \mu\text{J}/\text{cm}^2$ for $\hbar\omega_{\text{P}} = 1.55$ eV and 3.1 eV, respectively, (a), (b) and at $\mathcal{F} = 17.4 \mu\text{J}/\text{cm}^2$ and $15 \mu\text{J}/\text{cm}^2$ for $\hbar\omega_{\text{P}} = 1.55$ eV and 3.1 eV, respectively (c), (d). For comparison amplitudes in a slightly higher T_{c} sample are shown in (b), (d). The thin line in (c) is the fit of equation (5) to the data.

ternal fluence, \mathcal{F}_{T} , at which the superconductivity is destroyed in the most excited spot of the pump beam. From \mathcal{F}_{T} we calculate, using optical penetration depths, λ_{op} , and reflectivities, R , of $\text{LaAsFeO}_{1-x}\text{F}_x$,⁴⁴ the energy density, U_{p} , required to completely destroy the superconducting state: $U_{\text{p}}/k_{\text{B}} = \mathcal{F}_{\text{T}}(1-R)/\lambda_{\text{op}}k_{\text{B}} = 2.2 \text{ K/Fe}$ ($U_{\text{p}} = 18 \text{ J/mol}$) at $\hbar\omega_{\text{P}} = 3.1$ eV and $U_{\text{p}}/k_{\text{B}} = 1.5 \text{ K/Fe}$ ($U_{\text{p}} = 12 \text{ J/mol}$) at $\hbar\omega_{\text{P}} = 1.55$ eV. The average value $U_{\text{p}}/k_{\text{B}} = 1.8 \text{ K/Fe}$ is slightly smaller than the values observed in $\text{La}_{1-x}\text{Sr}_x\text{CuO}_4$.³¹ If we assume that the thermodynamic superconducting condensation energy, U_{c} , in $\text{SmFeAsO}_{0.8}\text{F}_{0.2}$ is similar to $\text{La}_{1-x}\text{Sr}_x\text{CuO}_4$ due to similar magnitudes of T_{c} we obtain $U_{\text{p}}/U_{\text{c}} \gg 1$ indicating that a significant amount of excitation energy is transferred to the bath on a timescale of ~ 0.3 ps. If all degrees of freedom would absorb U_{p} the resulting temperature rise would be 11K based on the published heat capacity, c_{p} , data⁴⁵. Contrary to the cuprates c_{p} is dominated by Sm spins^{45,46} below ~ 12 K so it is not possible to determine whether the excess U_{p} is absorbed in the Sm-spin or in the phonon subsystem.

We fit the temperature dependence of the reflectivity change upon complete destruction of the superconducting state shown in Fig. 11 (d) by the high-frequency limit

of the Mattis-Bardeen formula,⁴⁷

$$\frac{\Delta R}{R} \propto \left(\frac{\Delta(T)}{\hbar\omega} \right)^2 \log \left(\frac{3.3\hbar\omega}{\Delta(T)} \right), \quad (5)$$

where $\hbar\omega$ is the probe-photon energy and $\Delta(T)$ the superconducting gap. By using the BCS-gap temperature dependence with $2\Delta_0/k_B T_c = 3.5$ we obtain an excellent fit to the observed temperature dependence. Unfortunately the shape of the temperature dependence (5) is a very weak function of $2\Delta_0/k_B T_c$ and one can not reliably distinguish the contributions from different gaps⁴⁸ and reliably determine $2\Delta_0/k_B T_c$.

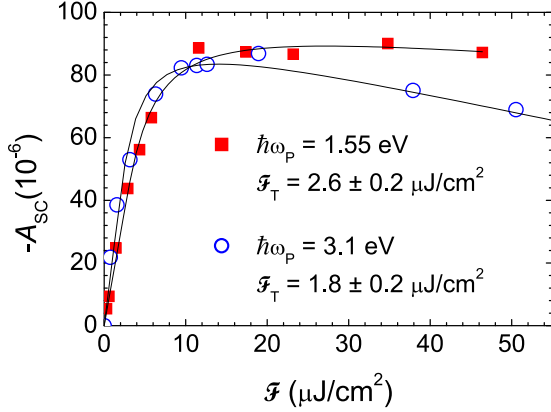


Figure 12: The amplitude of the component C as functions of fluence at different $\hbar\omega_p$. Thin lines are fits discussed in text.

D. Normal state response in $\text{SmFeAsO}_{0.8}\text{F}_{0.2}$

The temperature dependence of the component-B amplitude is consistent with a bottleneck due to the relaxation over a T -independent gap¹⁶ (see Fig. 9) with a magnitude $2\Delta_{PG} = 120$ meV as noted previously.⁴¹ The sub-ps part of component A on the other hand is temperature independent suggesting finite density of states at ϵ_F . This is consistent with heat capacity measurements in polycrystalline $\text{SmFeAsO}_{1-x}\text{F}_x$ ^{45,46} where a finite Sommerfeld constant in the superconducting state suggests a finite density of states at ϵ_F . Due to very similar pump-photon energy dispersion of components A and B we believe that they originate from the same electronic states which have a soft-gapped density of states at ϵ_F . Saturation of component B amplitude with increasing \mathcal{F} indicates that the pseudogap can be destroyed so it is not a simple band-structure effect.

The pump-photon energy dispersion similar to that of components A and B is not observed for component C. Electronic states involved in the relaxation related to components A and B must therefore be different than for component C. This confirms that the relaxation below T_c does *not* proceed via a cascade but rather through distinct parallel channels as suggested previously.⁴¹ These

channels correspond to two distinct electronic subsystems which are weakly coupled on the sub-ps timescale. One exhibits the superconducting gap(s) and the other a pseudogap.

A possible origin of the distinct electronic subsystems could be a chemical phase separation of the doped F. However, the superconducting transition is rather narrow (see Fig. 4) so the presence of weakly-superconducting fluorine-poor regions in which SDW is suppressed giving rise to additional pseudo-gapped electronic subsystem is also unlikely. More importantly undoped SmFeAsO shows virtually no pump-photon energy dispersion which the superconducting sample does, so a simple chemical phase separation to doped and undoped regions is very unlikely despite similarity (see Fig. 6) between component A and the undoped SmFeAsO room-temperature transients. Moreover, there is no divergent signal at 125 K (or anywhere near that temperature) which can be attributed to the presence of the undoped phase in the superconducting sample. We therefore believe that both electronic subsystems are intrinsic to the SC material.

Apart from the chemical phase separation an intrinsic electronic phase separation akin to that proposed for the cuprates⁴⁹ could be origin of the distinct electronic subsystems. The existence of intrinsic electronic phase separation has been reported in 122 systems,^{50,51} however at present the issue is still rather controversial.

In the case of the spatially homogeneous electronic state different electronic subsystems would correspond to different bands crossing ϵ_F . This would imply that the inter-band scattering between parts of the Fermi surface corresponding to different electronic subsystems is negligible on a timescale of a few hundred fs, since excitation photon at 1.5 eV only weakly excites components A and B. Further, since both components exist in the superconducting state even at low \mathcal{F} the part of the Fermi surface corresponding to components A and B has to remain ungapped or pseudo-gapped in the superconducting state.

Another possibility for a weakly coupled electronic subsystem are Sm crystal-field levels. The energy of the levels in $\text{SmFeAsO}_{1-x}\text{F}_x$ is in the range of 20-60 meV as determined indirectly from heat capacity fits.^{52,53} Involvement of the crystal-field levels could explain the strong $\hbar\omega_p$ -dependence of components A and B and decoupling from the other low lying electronic states. However, the observation of a pseudogap by NMR in La-1111 ^{12,13} (which has no crystal field level structure at low energy), and the weak $\hbar\omega_p$ -dependence in undoped SmFeAsO point against such a scenario.

Finally, let us briefly compare our results in Sm-1111 to femtosecond spectroscopy in $(\text{Ba,K})\text{-122}$.^{54,55} There is a marked difference in the magnitude of the relaxation time in the superconducting state, which increases with decreasing temperature beyond 60 ps in optimally doped $(\text{Ba,K})\text{-122}$ ⁵⁴ and remains T -independent in Sm-1111 at ~ 5 ps. Similarly, the excitation fluence dependence of the relaxation time, which is absent in Sm-1111 is pronounced in $(\text{Ba,K})\text{-122}$.⁵⁵ This suggests different relax-

ation mechanisms in Sm-1111 and (Ba,K)-122. While behavior in (Ba,K)-122 is consistent with the Rotwarf-Taylor model^{27,56} where the anharmonic optical-phonon decay is determining the relaxation time in Sm-1111 the presence of the ungapped electronic subsystem seems to provide a competing relaxation channel. However, only $\hbar\omega_P = 1.55$ eV was used in (Ba,K)Fe₂As₂ so ultrafast pump-probe spectroscopy at different $\hbar\omega_P$ in 122 systems and measurements in LaFeAsO_{1-x}F_x are needed for determination whether some fundamental difference between 1111 and 122 systems is responsible for the different relaxation time behavior and marked temperature dependence above T_c in Sm-1111.

III. SUMMARY AND CONCLUSIONS

In undoped SmFeAsO a single-exponential relaxation is observed. From the high- T relaxation time the second moment of the Eliashberg function is determined to be $\lambda\langle\omega^2\rangle = 135 \pm 10$ meV². The coupling constant $\lambda \approx 0.2$, estimated from this value, is comparable to low- T_c superconductors and cannot explain the high superconducting T_c s of these compounds within a single band BCS model.

Below T_{SDW} the temperature dependence of the relaxation indicates appearance of a QP relaxation bottleneck due to opening of a single charge gap at T_{SDW} with a BCS-like temperature dependence and the amplitude of $2\Delta_{SDW}/k_B T_{SDW} \simeq 5$ at 4.2 K. A question whether this charge gap is a direct consequence of the SDW formation or due to the structural transition unfortunately cannot be answered from our data.

In superconducting SmFeAsO_{0.8}F_{0.2} three distinct relaxation components are observed. Components A and B are present in both the superconducting and the normal state. The temperature dependence of the amplitude

of component B suggests the presence of a temperature independent pseudogap with a magnitude $2\Delta_{PG} \simeq 120$ meV. The pseudogap is destroyed at a finite fluence indicating that it is not a band-structure effect (such as a 120 meV gap at some arbitrary point in the Brillouin zone). Component C is observed only in the superconducting state and corresponds to the relaxation across a T -dependent superconducting gap with a BCS temperature dependence. At high enough pump fluence a complete destruction of the superconducting state is observed with the critical optical excitation density $U_P/k_B \approx 1.8$ K/Fe which is similar to the value observed in (La,Sr)CuO₄.

The multicomponent relaxation in SC samples strongly suggest the presence of two relatively weakly coupled electronic subsystems, one exhibiting the SC gap(s) and the other the pseudogap. From the temperature and fluence dependence of photoinduced optical reflectivity transients in undoped and near-optimally doped SmFeAsO_{1-x}F_x single crystals it is clear that the presence of two electronic subsystems in the superconducting sample is not a result of a simple phase separation. The fact that no relaxation component - such as appears in the SDW phase - is seen in the SC phase appears to rule this out. The presence of two electronic subsystems therefore originates either in an intrinsic phase separation or more likely in the multiband nature of the superconducting iron-pnictides.

Acknowledgments

This work has been supported by ARRS (GrantNo.P1-0040) and the Swiss National Science Foundation NCCR MaNEP.

-
- ¹ Y. Kamihara, H. Hiramatsu, M. Hirano, R. Kawamura, H. Yanagi, T. Kamiya, and H. Hosono, *Journal of the American Chemical Society* **128**, 10012 (2006), URL <http://dx.doi.org/10.1021/ja063355c>.
 - ² Y. Kamihara, T. Watanabe, M. Hirano, H. Hosono, et al., *J. Am. Chem. Soc.* **130**, 3296 (2008).
 - ³ Z. Ren, G. Che, X. Dong, J. Yang, W. Lu, W. Yi, X. Shen, Z. Li, L. Sun, F. Zhou, et al., *EPL-Europhysics Letters* **83**, 17002 (2008).
 - ⁴ D. J. Singh and M.-H. Du, *Physical Review Letters* **100**, 237003 (pages 4) (2008), URL <http://link.aps.org/abstract/PRL/v100/e237003>.
 - ⁵ A. I. Coldea, J. D. Fletcher, A. Carrington, J. G. Analytis, A. F. Bangura, J.-H. Chu, A. S. Erickson, I. R. Fisher, N. E. Hussey, and R. D. McDonald, *Physical Review Letters* **101**, 216402 (pages 4) (2008), URL <http://link.aps.org/abstract/PRL/v101/e216402>.
 - ⁶ W. Hu, J. Dong, G. Li, Z. Li, P. Zheng, G. Chen, J. Luo, and N. Wang, *Phys Rev Lett* **101**, 257005 (2008).
 - ⁷ Z. Chen, R. Yuan, T. Dong, N. Wang, S. Ce, N. Pr, et al.,

- Arxiv preprint arXiv:0910.1318 (2009).
- ⁸ H. Ding, P. Richard, K. Nakayama, K. Sugawara, T. Arakane, Y. Sekiba, A. Takayama, S. Souma, T. Sato, T. Takahashi, et al., *EPL (Europhysics Letters)* **83**, 47001 (2008).
- ⁹ S. Kawasaki, K. Shimada, G. F. Chen, J. L. Luo, N. L. Wang, and G. qing Zheng, *Physical Review B (Condensed Matter and Materials Physics)* **78**, 220506 (pages 4) (2008), URL <http://link.aps.org/abstract/PRB/v78/e220506>.
- ¹⁰ D. Daghero, M. Tortello, R. S. Gonnelli, V. A. Stepanov, N. D. Zhigadlo, and J. Karpinski, *Physical Review B (Condensed Matter and Materials Physics)* **80**, 060502 (pages 4) (2009), URL <http://link.aps.org/abstract/PRB/v80/e060502>.
- ¹¹ C. Martin, M. E. Tillman, H. Kim, M. A. Tanatar, S. K. Kim, A. Kreyssig, R. T. Gordon, M. D. VanNette, S. Nandi, V. G. Kogan, et al., *Physical Review Letters* **102**, 247002 (pages 4) (2009), URL <http://link.aps.org/abstract/PRL/v102/e247002>.

- ¹² K. Ahilan, F. L. Ning, T. Imai, A. S. Sefat, R. Jin, M. A. McGuire, B. C. Sales, and D. Mandrus, *Physical Review B (Condensed Matter and Materials Physics)* **78**, 100501 (pages 4) (2008), URL <http://link.aps.org/abstract/PRB/v78/e100501>.
- ¹³ Y. Nakai, S. Kitagawa, K. Ishida, Y. Kamihara, M. Hirano, and H. Hosono, *New Journal of Physics* **11**, 045004 (2009).
- ¹⁴ R. Gonnelli, D. Daghero, M. Tortello, G. Ummarino, V. Stepanov, R. Kremer, J. Kim, N. Zhigadlo, and J. Karpinski, *Physica C: Superconductivity* **469**, 512 (2009), ISSN 0921-4534, superconductivity in Iron-Pnictides, URL <http://www.sciencedirect.com/science/article/B6TVJ-4VWB19T-B42f56028a17ed607285f01b706f035d4>.
- ¹⁵ C. J. Stevens, D. Smith, C. Chen, J. F. Ryan, B. Podobnik, D. Mihailovic, G. A. Wagner, and J. E. Evetts, *Phys. Rev. Lett.* **78**, 2212 (1997).
- ¹⁶ V. V. Kabanov, J. Demsar, B. Podobnik, and D. Mihailovic, *Phys. Rev. B* **59**, 1497 (1999).
- ¹⁷ J. Demsar, B. Podobnik, V. V. Kabanov, T. Wolf, and D. Mihailovic, *Phys. Rev. Lett.* **82**, 4918 (1999).
- ¹⁸ R. Kaindl, M. Woerner, T. Elsaesser, D. Smith, J. Ryan, G. Farnan, M. McCurry, and D. Walmsley, *Science* **287**, 470 (2000).
- ¹⁹ D. Dvorsek, V. V. Kabanov, J. Demsar, S. M. Kazakov, J. Karpinski, and D. Mihailovic, *Phys. Rev. B* **66**, 020510 (2002).
- ²⁰ G. P. Segre, N. Gedik, J. Orenstein, D. A. Bonn, R. Liang, and W. N. Hardy, *Phys. Rev. Lett.* **88**, 137001 (2002).
- ²¹ M. Schneider, J. Demsar, Y. Glinka, A. Klimov, A. Krapf, S. Rast, Y. Ren, et al., *EPL (Europhysics Letters)* **60**, 460 (2002).
- ²² J. Demsar, R. D. Averitt, A. J. Taylor, V. V. Kabanov, W. N. Kang, H. J. Kim, E. M. Choi, and S. I. Lee, *Phys. Rev. Lett.* **91**, 267002 (2003).
- ²³ N. Gedik, J. Orenstein, R. Liang, D. Bonn, and W. Hardy, *Science* **300**, 1410 (2003).
- ²⁴ N. Gedik, P. Blake, R. C. Spitzer, J. Orenstein, R. Liang, D. A. Bonn, and W. N. Hardy, *Phys. Rev. B* **70**, 014504 (2004).
- ²⁵ P. Kusar, J. Demsar, D. Mihailovic, and S. Sugai, *Phys. Rev. B* **72**, 014544 (2005).
- ²⁶ R. A. Kaindl, M. A. Carnahan, D. S. Chemla, S. Oh, and J. N. Eckstein, *Phys. Rev. B* **72**, 060510 (2005).
- ²⁷ V. V. Kabanov, J. Demsar, and D. Mihailovic, *Phys. Rev. Lett.* **95**, 147002 (2005).
- ²⁸ G. Bianchi, C. Chen, M. Nohara, H. Takagi, and J. F. Ryan, *Phys. Rev. B* **72**, 094516 (2005).
- ²⁹ M. L. Schneider, M. Onellion, X. X. Xi, X. Zeng, A. Soukiasian, P. Omernik, and G. Taft, *Phys. Rev. B* **70**, 012504 (2004).
- ³⁰ V. V. Kabanov and A. S. Alexandrov, *Physical Review B (Condensed Matter and Materials Physics)* **78**, 174514 (pages 8) (2008), URL <http://link.aps.org/abstract/PRB/v78/e174514>.
- ³¹ P. Kusar, V. Kabanov, J. Demsar, T. Mertelj, S. Sugai, and D. Mihailovic, *Physical Review Letters* **101**, 227001 (2008).
- ³² N. Zhigadlo, S. Katrych, Z. Bukowski, S. Weyeneth, R. Puzniak, and J. Karpinski, *J. Phys.: Condens. Matter* **20**, 342202 (2008).
- ³³ V. G. Hadjiev, M. N. Iliev, K. Sasmal, Y.-Y. Sun, and C. W. Chu, *Physical Review B (Condensed Matter and Materials Physics)* **77**, 220505 (pages 3) (2008), URL <http://link.aps.org/abstract/PRB/v77/e220505>.
- ³⁴ H.-H. Klauss, H. Luetkens, R. Klingeler, C. Hess, F. J. Litterst, M. Kraken, M. M. Korshunov, I. Eremin, S.-L. Drechsler, R. Khasanov, et al., *Physical Review Letters* **101**, 077005 (pages 4) (2008), URL <http://link.aps.org/abstract/PRL/v101/e077005>.
- ³⁵ A. Drew, C. Niedermayer, P. Baker, F. Pratt, S. Blundell, T. Lancaster, R. Liu, G. Wu, X. Chen, I. Watanabe, et al., *Nature materials* (2009).
- ³⁶ S. Margadonna, Y. Takabayashi, M. McDonald, M. Brunelli, G. Wu, R. Liu, X. Chen, and K. Prasad, *Physical Review B* **79**, 14503 (2009).
- ³⁷ S. Sanna, R. De Renzi, G. Lamura, C. Ferdeghini, T. Shiroka, *Physical Review B* **80**, 52503 (2009).
- ³⁸ H. Luo, Z. Wang, H. Yang, P. Cheng, X. Zhu, and H. Wen, *Supercond. Sci. Technol* **21**, 125014 (2008).
- ³⁹ C. Gadermaier, A. S. Alexandrov, V. V. Kabanov, P. Kusar, T. Mertelj, X. Yao, C. Manzoni, G. Cerullo, and D. Mihailovic, *ArXiv e-prints* (2009), 0902.1636.
- ⁴⁰ R. Osborn, S. Rosenkranz, E. Goremychkin, and A. Christianson, *Physica C: Superconductivity and its applications* **469**, 498 (2009).
- ⁴¹ T. Mertelj, V. Kabanov, C. Gadermaier, N. Zhigadlo, S. Katrych, J. Karpinski, and D. Mihailovic, *Physical Review Letters* **102**, 117002 (2009).
- ⁴² T. Mertelj, V. Kabanov, C. Gadermaier, N. Zhigadlo, S. Katrych, Z. Bukowski, J. Karpinski, and D. Mihailovic, *Journal of Superconductivity and Novel Magnetism* **22**, 575 (2009).
- ⁴³ D. Mihailovic and J. Demsar, *Spectroscopy of Superconducting Materials* (American Chemical Society: Washington, DC, 1999), vol. 730 of *ACS Symposium Series*, chap. Time-resolved optical studies of quasiparticle dynamics in high-temperature superconductors, pp. 230–244.
- ⁴⁴ A. V. Boris, N. N. Kovaleva, S. S. A. Seo, J. S. Kim, P. Popovich, Y. Matiks, R. K. Kremer, and B. Keimer, *Physical Review Letters* **102**, 027001 (pages 4) (2009), URL <http://link.aps.org/abstract/PRL/v102/e027001>.
- ⁴⁵ M. Tropeano, A. Martinelli, A. Palenzona, E. Bellingeri, E. G. d'Aglano, T. D. Nguyen, M. Affronte, and M. Putti, *Physical Review B (Condensed Matter and Materials Physics)* **78**, 094518 (pages 7) (2008), URL <http://link.aps.org/abstract/PRB/v78/e094518>.
- ⁴⁶ L. Ding, C. He, J. K. Dong, T. Wu, R. H. Liu, X. H. Chen, and S. Y. Li, *Physical Review B (Condensed Matter and Materials Physics)* **77**, 180510 (pages 4) (2008), URL <http://link.aps.org/abstract/PRB/v77/e180510>.
- ⁴⁷ D. C. Mattis and J. Bardeen, *Phys. Rev.* **111**, 412 (1958).
- ⁴⁸ J. Karpinski, N. Zhigadlo, S. Katrych, Z. Bukowski, P. Moll, S. Weyeneth, H. Keller, R. Puzniak, M. Tortello, D. Daghero, et al., *Physica C: Superconductivity* **469**, 370 (2009), ISSN 0921-4534, superconductivity in Iron-Pnictides, URL <http://www.sciencedirect.com/science/article/B6TVJ-4VWB19T-4>.
- ⁴⁹ L. Gor'kov, *Journal of Superconductivity* **14**, 365 (2001).
- ⁵⁰ J. T. Park, D. S. Inosov, C. Niedermayer, G. L. Sun, D. Haug, N. B. Christensen, R. Dinnebier, A. V. Boris, A. J. Drew, L. Schulz, et al., *Physical Review Letters* **102**, 117006 (pages 4) (2009), URL <http://link.aps.org/abstract/PRL/v102/e117006>.
- ⁵¹ Y. Laplace, J. Bobroff, F. Rullier-Albenque, D. Colson, and A. Forget, *Physical Review B (Condensed Matter and Materials Physics)* **80**, 140501 (pages 4) (2009), URL

- <http://link.aps.org/abstract/PRB/v80/e140501>.
- ⁵² R. Cimperle, C. Ferdeghini, F. Canepa, M. Ferretti, A. Martinelli, A. Palenzona, A. Siri, and M. Tropeano, Arxiv preprint arXiv:0807.1688 (2008).
 - ⁵³ P. Baker, S. Giblin, F. Pratt, R. Liu, G. Wu, X. Chen, M. Pitcher, D. Parker, S. Clarke, and S. Blundell, *New Journal of Physics* **11**, 5010 (2009).
 - ⁵⁴ E. E. M. Chia, D. Talbayev, J. Zhu, H. Q. Yuan, T. Park, J. D. Thompson, G. F. Chen, J. L. Luo, N. L. Wang, and A. J. Taylor, ArXiv e-prints (2008), 0809.4097.
 - ⁵⁵ D. H. Torchinsky, G. F. Chen, J. L. Luo, N. L. Wang, and N. Gedik, ArXiv e-prints (2009), 0905.0678.
 - ⁵⁶ A. Rothwarf and B. N. Taylor, *Phys. Rev. Lett.* **19**, 27 (1967).
 - ⁵⁷ K. Ishida, Y. Nakai, H. Hosono, Y. Kuramoto, H. Kusunose, A. Kiss, R. Kubo, M. Fujita, K. Wakabayashi, K. Nakada, et al., *J. Phys. Soc. Jpn* **78**, 062001 (2009).
 - ⁵⁸ For a recent review see ref. 57.